Appl Water Sci (2016) 6:319–330
DOI 10.1007/s13201-014-0227-1

ORIGINAL ARTICLE

Thermodynamic and kinetic studies of biosorption of iron and manganese from aqueous medium using rice husk ash

F. A. Adekola · D. S. S. Hodonou · H. I. Adegoke

Received: 10 December 2013 / Accepted: 21 July 2014 / Published online: 26 November 2014

Abstract The adsorption behavior of rice husk ash with respect to manganese and iron has been studied by batch methods to consider its application for water and waste water treatment. The optimum conditions of adsorption were determined by investigating the effect of initial metal ion concentration, contact time, adsorbent dose, pH value of aqueous solution and temperature. Adsorption equilibrium time was observed at 120 min. The adsorption efficiencies were found to be pH dependent. The equilibrium adsorption experimental data were found to fit the Langmuir, Freundlich and Temkin isotherms for iron, but fitted only Langmuir isotherm for manganese. The pseudo-second order kinetic model was found to describe the manganese and iron kinetics more effectively. The thermodynamic experiment revealed that the adsorption processes involving both metals were exothermic. The adsorbent was finally applied to typical raw water with initial manganese and iron concentrations of 3.38 mg/l for Fe and 6.28 mg/l, respectively, and the removal efficiency was 100 % for Mn and 70 % for Fe. The metal ions were desorbed from the adsorbent using 0.01 M HCl, it was found to quantitatively remove 67 and 86 % of Mn and Fe, respectively, within 2 h. The results revealed that manganese and iron are considerably adsorbed on the adsorbent and could be an economic method for the removal of these metals from aqueous solutions.

Keywords Thermodynamics · Kinetics · Biosorption · Rice husk ash · Isotherms

F. A. Adekola · D. S. S. Hodonou · H. I. Adegoke (✉)
Department of Chemistry, University of Ilorin, Ilorin, Nigeria
e-mail: adegoke.hi@unilorin.edu.ng

F. A. Adekola
e-mail: fadekola@unilorin.edu.ng

Introduction

Water pollution is a major global problem which requires ongoing evaluation and revision of water resource policy at all levels (international down to individual aquifers and wells). It has been suggested that it is the leading worldwide cause of deaths and diseases, and that it accounts for the deaths of more than 14,000 people daily. The contamination of both surface and groundwater by heavy metals constitutes an environmental hazard due to the fact that metals are not biodegradable and can cause severe adverse effects on human health (Spellman 2001).

The presence of iron and manganese compounds, in groundwater, and eventually in drinking water, is a serious environmental problem which poses a substantial risk to local resource user and to the natural environment. Many techniques have been developed for removing heavy metals from water and wastewater and these include polyphosphate treatment, ion-exchange treatment, precipitations, ultra filtration and chlorination (Bruce Seelig 1998). Recently the uses of some natural biomaterials as adsorbents have been advocated. The advantages of biosorbents include low operational cost and biodegradability. Biomaterials that have been used to remove heavy metals from aqueous solution include rice husk carbon, phosphate-treated rice husk, and rice husk carbon, *Moringa* seeds (Jahn 1988). Sari et al. in their study reported the biosorption characteristics of Cd (II) and Cr(III) ions from aqueous solution using moss (*Hylocomium splendens*) biomass. In their report, experimental data fitted into Langmuir model better than Freundlich isotherm. The calculated thermodynamic parameters showed that the biosorption of the metal ions studied onto the biomass was feasible, spontaneous and exothermic under examined conditions (Sari et al. 2008). In another related study,

biosorption characteristics of Pb(II) and Cd (II) ions from aqueous solution using microfungus (*Amanita rubescens*) biomass were investigated as a function of pH, contact time, temperature and some other parameters. The biosorption of the metal ions by *Amanita rubescens* fitted into Langmuir model better than Freundlich isotherm (Sari and Tuzen 2009).

The main objective of this study is to investigate the potential use of rice husk ash, an agricultural waste material as low cost bio-adsorbent for removal of iron and manganese ions from aqueous solution and real raw water from a local dam. The effect of some physical–chemical and thermodynamic parameters such as pH, adsorbent dose, temperature, ionic strength, the effect of initial concentration, the effect of contact time on the sorption capacity were investigated.

Materials and methods

Collection of rice husk waste material

Rice-husk, an agro-residue waste material was collected from a processing center at a local market in Ilorin, Kwara State of Nigeria.

Preparation of adsorbents

The rice husk (RH) was milled and later washed with distilled water to remove all impurities. The material was then oven dried at 105 °C for 5–6 h. It was thereafter sieved and the fraction with particle size $300 < \phi < 250$ μm was selected for further pretreatment. The RH was purified in 500 ml of 0.3 M of HNO_3 (Merck South Africa) over night and mechanically stirred at moderate speed; it was then washed thoroughly with large quantity of distilled water to neutrality and subsequently air dried at 105 °C for 24 h (Laurence and Christopher 1989; Abdullah et al. 2001). The material was ashed at 550 °C in the muffle furnace and labeled, Ash-RH.

Characterization of adsorbents

The specific surface area was determined using Sears' method (Shawabkeh et al. 2003).

The elemental composition of the adsorbent was determined using X-ray fluorescence (XRF) spectrometry.

The major functional groups in the adsorbent were determined by Fourier transform infrared spectrometry (FTIR-8400S). It was used to determine the functional groups in the samples at wave number 400–4,000 cm^{-1}.

The pH of the adsorbent was determined by weighing 1 g of Ash-RH, boiled in a beaker containing 100 ml of distilled water for 5 min. The solution was diluted to 200 ml with distilled water and cooled at room temperature, the pH of each was measured using a pH meter (model ATPH-6) and the readings were recorded (Abdullah et al. 2001).

The bulk density of Ash-RH was determined using Archimedes's principle. The bulk density was determined using the equation below (Toshiguki and Yukata 2003).

$$\text{Bulk density} = \frac{W_2 - W_1}{V}$$

where W_1, is the weight of empty measuring cylinder, W_2 is the weight of cylinder filled with sample and V is the volume of cylinder.

The turbidity of the adsorbent particles suspension in aqueous media was used to evaluate the rate of agglomeration and sedimentation of rice husks ash (Ash-RH) particles. The turbidity study of the adsorbent was carried out to determine the influence of pH on the sedimentation behavior of the adsorbent particles. The study was carried out by varying the pH of colloidal suspension of 0.1 g biosorbent in 20 ml of aqueous solution between 3 and 7. The turbidity value was measured at various time intervals using a HACH turbidimeter model 2,100 N.

Batch adsorption experiments

The adsorption experiments were conducted using 0.1 g of Ash-RH with 20 ml of solutions containing heavy metal ions of desired concentrations at constant temperature of 30 ± 2 °C in 100 ml plastic bottles. The mixtures were shaken on a shaker for 5 h and mixtures were filtered through Whatman filter paper No 1. The exact concentrations of metal ions in the initial and final solution were determined spectrophotometrically. The percent (%) adsorbed was calculated using the equation below (Uberoi et al. 1990).

$$\%\ \text{Adsorption} = \frac{C_0 - C_e}{C_0} \times 100$$

where C_0 and C_e are the initial and final concentrations of the metal ions in solution, respectively.

Adsorption isotherms studies

The experimental data were fitted using Langmuir (Hall et al. 1966) Freundlich (Hutson and Yang 1997) and Temkin adsorption isotherms.

The Langmuir isotherm equation is written as:

$$\frac{C_e}{q_e} = \frac{1}{q_{max} K_L} + \frac{C_e}{q_{max}}$$

where C_e is the equilibrium concentration of adsorbate (mg/l^{-1}) and q_e is the amount of metal adsorbed per gram of the adsorbent at equilibrium (mg/g). q_m (mg/g) and b (l/mg) are Langmuir constants related to adsorption capacity and rate of adsorption, respectively. The values of q_m and b were calculated from the slope and intercept of the Langmuir plot of C_e versus C_e/q_e (Langmuir 1918).

Freundlich isotherm describes an empirical relationship that exists between the adsorption of solute and the surface of the adsorbent. This isotherm could be effectively utilized to study the heterogeneity and surface energies. The empirical equation proposed by Freundlich is:

$$q = K_f C^{1/n}$$

where, K_f and n are coefficients; q is the weight adsorbed per unit weight of adsorbent; C is the concentration of the metal solution

Taking logarithm and rearranging: $\log q = \log K_f + \frac{1}{n}\log C$

The constant K_f is an approximate indicator of adsorption capacity, while $1/n$ is a function of the strength of adsorption in the adsorption process. These constants can be evolved by linearising the above equation by adopting mathematical techniques (Voudrias et al. 2002).

If n is equal to 1 then the partition between the two phases is independent of the concentration. If the $1/n$ value is below 1 it indicates a normal adsorption. On the other hand if $1/n$ is above 1 it indicates cooperative adsorption (Mohan and Karthikeyan 1997).

Temkin adsorption isotherm

The Temkin isotherm model assumes that the adsorption energy decreases linearly with the surface coverage due to adsorbent–adsorbate interactions. The Temkin isotherm equation is applied for isotherm analysis in the following form (Temkin and Pyzhev 1940):

$$q_e = B\ln A + B\ln C_e$$

where C_e is the equilibrium concentration of adsorbate (mg/l^{-1}) and q_e is the amount of metal adsorbed per gram of the adsorbent at equilibrium (mg/g).

According to Temkin isotherm, the linear form can be expressed by equation

$$q_e = \frac{RT}{b}\ln K_T + \frac{RT}{b}\ln C_e$$

where $RT/b = B$ (J/mol), which is the Temkin constant related to heat of sorption, whereas K_T (l/g) represents the equilibrium binding energy, R (8.314 J/mol/K) is the universal gas constant at T (K) which is the absolute solution temperature.

Adsorption kinetics studies

The pseudo-first order and pseudo-second order models have been tested on the experimental data at different contact time. The pseudo-first order model is expressed using this equation (Ho et al. 1996)

$$\log(q_e - q) = \log q_e - \frac{K_{ad}}{2.303} \times t$$

where q_e (mg/g) is the mass of metal adsorbed at any time t and k_1 (min^{-1}) is the equilibrium rate constant of pseudo-first order adsorption. The values of k_{ad} and q_e are determined from the slope and intercept of the plot of log ($q_e - q_t$) versus t, respectively.

The pseudo-second order model is based on assumption that biosorption follows a second order mechanism. The rate of occupation of adsorption sites is proportional to the square of the number of unoccupied sites (Mckay and Ho 1999). The equation can be expressed as Ho and McKay (2002):

$$\frac{t}{q_t} = \frac{1}{k_2 q_e^2} + \frac{1}{q_e} \times t$$

where k_2 is the pseudo-second order rate constant (g/mg/min). The value of q_e is determined from the slope of the plot of t/q_t versus t.

Thermodynamic study

The thermodynamic parameters were obtained by varying the temperature conditions between 30 and 50 °C while keeping other variables constant including metal concentration, pH, adsorbent dose, contact time. The values of the thermodynamic parameters such as ΔG^o, ΔH^o, and ΔS^o, were calculated using the expression described below (Khan et al. 2005):

The Gibb's free energy of the adsorption process is calculated (Voudrias et al. 2002)

$$\Delta G = -RT\ln K_d$$

where ΔG^o is the standard Gibb's free energy change for the adsorption (J/mol), R is the universal gas constant (8.314 J/mol/K) while T is the temperature (K). K_d is the distribution coefficient of the adsorbate The plot of ln K_d versus $1/T$ gives a straight line with the slope and the intercept giving values of ΔH^o and ΔS^o.

$$\ln K_d = \Delta S/R - \Delta H/RT$$

These values could be used to compute ΔG^o from the Gibb's relation,

$$\Delta G = \Delta H - T\Delta S$$

where K_d is the distribution coefficient of the adsorbate, and it is equal to q_e/C_e (l/g). T is the temperature (K), $R = 8.314 \times 10^{-3}$ kJ K^{-1} mol^{-1}, q_e is quantity of metal ion sorbed (mg/g) and C_e is the equilibrium concentration of metal ion solution (mg/l). ΔG was calculated from the equation at temperature of 303–323 K.

Synergetic effect of metals in binary solution

Understanding of the synergetic effect is important for evaluating the degree of interference posed by associated metal ions in adsorptive treatment of waste water. Binary adsorption of metal ions was conducted with the same operating conditions as for mono-component adsorption in terms of volume (20 ml), adsorbent dose 0.1 g, and agitation time of 2 h. The simultaneous adsorption of Mn(II) and Fe(II) ions from binary mixtures was also investigated at pH 5 and temperature of 30 ± 2 °C. The quantities adsorbed were determined by subtracting the quantity of the heavy metals in each filtrate from the initial quantity of heavy metal in each binary solution before contact.

Desorption experiment

The regeneration of the adsorbent was undertaken by carrying out batch desorption experiments.

Different concentrations of HCl (0.05, 0.1, 0.2 M) were contacted with the Mn(II) or Fe(II) presorbed adsorbent in different conical flasks and each suspension was equilibrated at different time intervals (10, 20, 30, 60 and 120 min). After equilibration, the mixtures were filtered and filtrates were analyzed for the amount of Mn(II) and Fe(II) in the solution. A graph of the percentage desorbed was plotted against time.

Desorption index

The desorption index was used to determine the degree of the reversibility of the sorption process. It is the ratio of the percent of total metal adsorbed after sorption to the percentage total left on the adsorbent after desorption.

Application of batch optimization conditions for the removal of Mn and Fe from untreated dam water

Untreated raw water was collected from Unilorin campus dam on 9 May 2012 and was appropriately preserved by acidifying with few drop of 0.5 M of HCl to prevent precipitation of the metal ions. The batch optimization conditions were applied for the removal of Mn and Fe in Unilorin dam water, after contact with the adsorbent Ash-RH.

Table 1 Physico-chemical properties of rice husk ash

Properties	Ash-RH
pH	7.1
Bulk density (g/ml)	0.3277
Particle size	$300 < \phi < 250$ μm
Surface area (m^2/g)	54.1

Table 2 Elemental composition of rice husk ash

Elements	Ash-RH
K (w%)	1.82 ± 0.0213
Ca (ppm)	903 ± 436
Mn (ppm)	23 ± 2
Fe (ppm)	126 ± 3
Cu (ppm)	3 ± 0
Zn (ppm)	13 ± 4
Ni (ppm)	5 ± 1

Results and discussion

The physical properties of the Ash-RH are summarized in the Table 1.

XRF elemental analysis

The elemental composition of Ash-RH biomass using XRF technique is summarized in Table 2. It shows that Ca and K are present as major elements; Fe exists as minor while Mn, Zn, Cu and Ni exist at trace levels.

Results of adsorption studies

Effect of initial concentration on adsorption of Fe(II) and Mn(II) ions

The results obtained are presented in Fig. 1. Two different behaviors were observed for iron and manganese, while the former exhibited a higher increase in the quantity of metal adsorbed with initial concentration, the latter showed a slight increase. The quantity adsorbed for Mn and Fe at 100 ppm was 3.21 and 18.84 mg/g, respectively. It is, therefore, evident that rice husk ash has higher capacity for iron than manganese. This may also be attributed to an increase in the driving force of the concentration gradient with the increase in the initial metal concentration (Kalavathy and Miranda 2010).

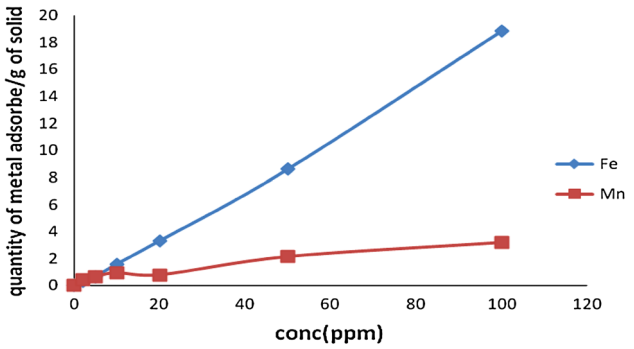

Fig. 1 Variation of initial metal ions concentration on the sorption capacity of iron and manganese: $m = 0.1$ g, $V = 20$ ml, time 7 h, temperature 30 °C

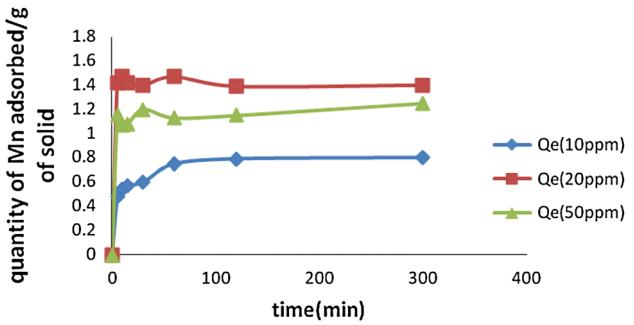

Fig. 2 Effect of contact time on the sorption of Mn(II) by Ash-RH ($m = 0.1$ g, $V = 20$ ml, pH 5, temperature of 30 °C, concentration 10–50 ppm)

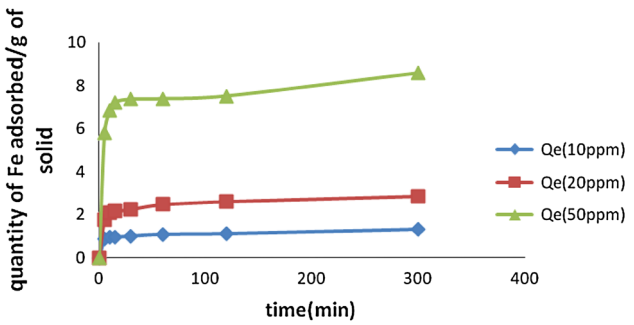

Fig. 3 Effect of contact time on the sorption of Fe(II) by Ash-RH ($m = 0.1$ g, $V = 20$ ml, pH 5, temperature of 30 °C, concentration 10–50 ppm)

Effect of contact time

The effect of contact time on adsorption is of importance in adsorption process, because of its influence on the adsorption capacity (Baysal 2009). The uptake of Mn(II) and Fe(II) ions were studied over a time range 5–300 min. The effect of contact time on removal efficiency is presented in Figs. 2 and 3. The results show that there is initial rapid increase in the quantity adsorbed within the first 10 min before approaching a plateau at about 100 min for Mn and 50 min for Fe. Subsequent experiment at concentrations 10, 20 and 50 ppm was carried out at 120 min (Figs. 4, 5, 6).

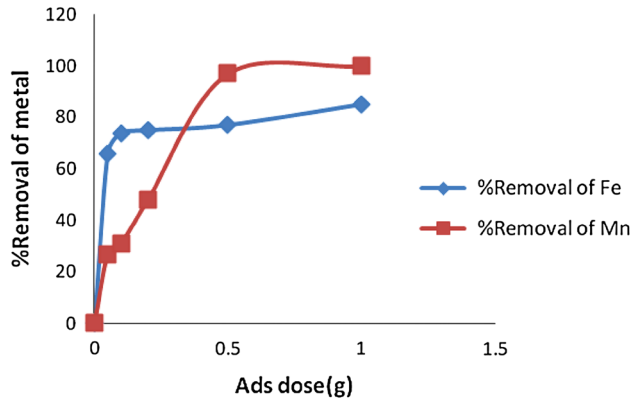

Fig. 4 Effect of adsorbent dose on % removal on the sorption of Mn(II) and Fe(II) on Ash-RH ($m = 0.1$ g, $V = 20$ ml, pH 5, temperature of 30 °C, concentration 10 ppm, time 120 min)

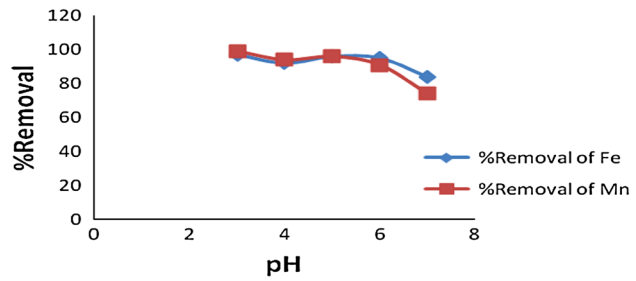

Fig. 5 Effect of pH on the percentage removal of Mn(II) and Fe(II) on Ash-RH [$m = 0.1$ g, $V = 20$ ml, pH (3–7), temperature from 30 °C, concentration 10 mg/l, time 120 min]

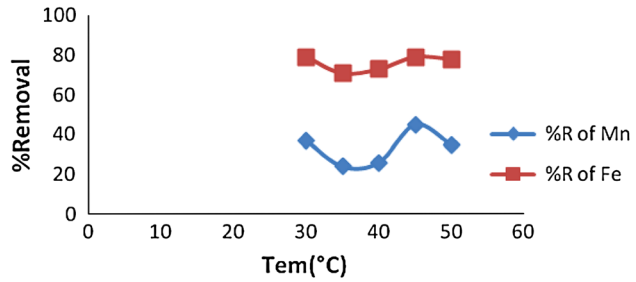

Fig. 6 Effect of temperature on the percentage removal of Mn(II) and Fe(II) on Ash-RH ($m = 0.1$ g, $V = 20$ ml, pH 5, temperature from 30 to 50 °C, concentration 10 mg/l, time 120 min)

Effect of adsorbent dose

The percent removal of both metals Mn(II) and Fe(II) increased with increase in Ash-RH dosage and attained a plateau (i.e. reached maximum amount) at 0.1 g for Fe and 0.5 g for Mn. The observed increase in the percent removal

of the metals with increase in dose of the adsorbent (Ash-RH particles) can be attributed to the increase in the surface area which leads to an increase in number of active sites for adsorption (Mckay and Ho 1999; Lakshminarayanan et al. 1994).This may also be due to an increase in effective surface area resulting from the conglomeration of the adsorbent especially at higher dosage of the adsorbent (Annadurai et al. 1997; Danis et al. 1999).

Effect of pH

The percentage removal was practically the same for the metal ions considered, as it varied between 92 and 97 % for Fe, and between 91 and 99 % for Mn at pH 3–6. The percentage removal, however, reduced to 84 % for Fe and 74 % for Mn when the pH was adjusted to 7. The effect of pH can be explained considering the surface charge on the adsorbent material. At low pH, due to high positive charge density and due to protons on the surface sites, during the uptake of metal ions electrostatic repulsion will be high, resulting in lower removal efficiency. Electrostatic repulsion decreases with increasing pH due to reduction of positive charge density on the sorption sites; thus an enhancement of metal adsorption is noted. Effect of pH on adsorption also has been reported by several earlier workers (Dubinin and Radushkevich 1947). At higher pH values OH^- ions compete with the metal ions with the active sites on the surface of the adsorbents.

Effect of temperature

The equilibrium uptake of Mn(II) and Fe(II) by 0.1 g of Ash-RH was slightly affected by temperature. The slight variation in equilibrium uptake was more pronounced in the case of manganese than iron. It was observed that the percentage removal was practically irregular with temperature. The decrease in adsorption with the rise of temperature may be due to the formation of the adsorbate–adsorbent complex which becomes unstable resulting in the escape from solid phase to the bulk solution. It is also likely that the instability of the complex may be accompanied by damage to the adsorption sites of the adsorbent thereby decreasing the metal ions uptake at higher temperature (Bhattacharyya and Gupta Sen 2006). The instability of the complex might also account for this downward and upward increase in the metal ions uptake.

Adsorption behavior of metals in binary solution

The respective concentrations of Mn(II) and Fe(II) in the experimental binary solutions used in this study are shown in Table 3.

Table 3 The respective concentrations of Mn(II) and Fe(II) in the experimental binary solutions

S/no	Mn (ppm)	Fe (ppm)
1	0	20
2	5	15
3	10	10
4	15	5
5	20	0

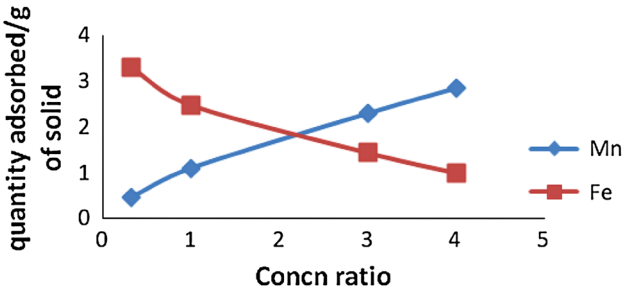

Fig. 7 Plot of adsorption behavior of Mn and Fe ions in a binary solution ($m = 0.1$ g, $V = 20$ ml, temp. 30 °C, pH 5, contact time 120 min)

Table 4 Thermodynamic parameters for manganese (II) and iron (II)

Metals	ΔG^o (kJ/mol)	ΔH^o (kJ/mol)	ΔS^o (J/mol/K)
Mn	−20285.76	−10492.77	32.11
Fe	−107824.62	−57499.628	165.28

Binary adsorption studies are important for assessing the degree of interference posed by common metal ions in adsorptive treatment of wastewaters and aqueous solutions (El-Said et al. 2010). Adsorbents generally exhibit three possible types of behavior and these are synergistic (the effect of the mixture is greater than that of the single components in the mixture), antagonism (the effect of the mixture is less than that of each of the components in the mixture) and non-interaction (the mixture has no effect on the adsorption of each of the adsorbates in the mixture) (Xiao and Thomas 2004).

The overriding effect of the binary mixture of Mn(II) and Fe(II) seems to be antagonistic in this case (Fig. 7). This is because the experimental equilibrium effect of the mixture is less than that of each of the components in the mixture. Similar results have been obtained by some authors.

Thermodynamics evaluation of adsorption process

The data obtained for the thermodynamic parameters for manganese and iron are presented in Table 4 in Fig. 8a, b.

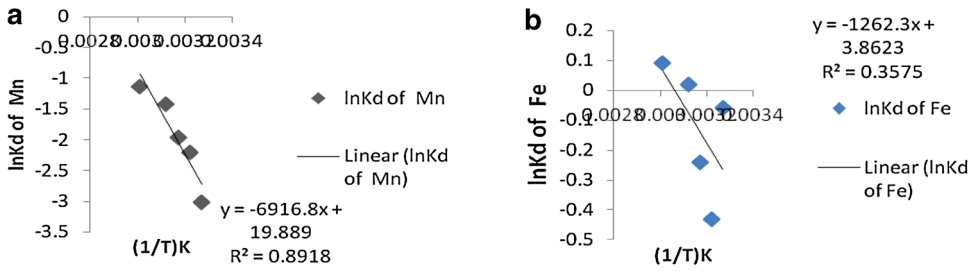

Fig. 8 **a** A plot of In K_d against $1/T$ (K^{-1}) for Mn(II) 10 ppm. **b** A plot of In K_d against $1/T$ (K^{-1}) for Fe(II) 10 ppm

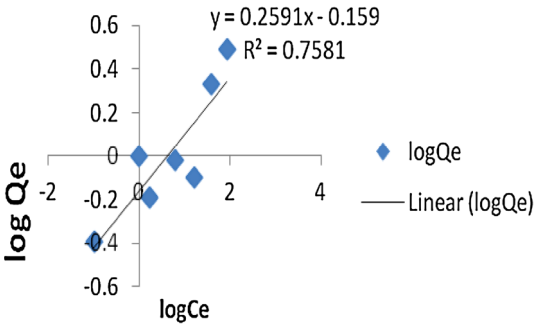

Fig. 9 Freundlich isotherm curve for manganese using Ash-RH at pH 5, temp. 30 °C, adsorbent dose 0.1 g

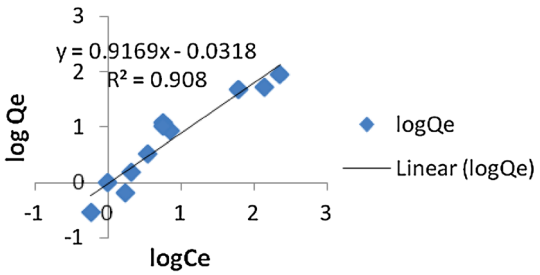

Fig. 10 Freundlich isotherm curve for manganese using Ash-RH at pH 5, temp. 30 °C, adsorbent dose 0.1 g

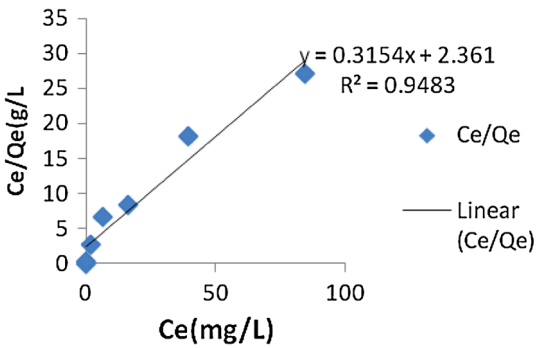

Fig. 11 Langmuir plot for sorption of Mn(II) ions on Ash-RH at pH 5, temp. 30 °C, adsorbent dose 0.1 g

The free energy change values obtained for the adsorption of Mn(II) and Fe(II) at 305 K, initial metal concentration of 10 ppm and pH 5 were −20,285.76 and −57,499.62 kJ mol^{-1}, respectively. This is confirmed by thermodynamic parameters such as free energy (ΔG^0, k cal mol^{-1}), enthalpy (ΔH^o, k cal mol^{-1}) and entropy (ΔS^o, cal mol^{-1} k^{-1}) changes during the process. These parameters were calculated at 305, 310, 315, 320 and 325 K temperatures (Singh et al. 1988). As the temperature increases, the values of ΔG become more negative for each metal (Malakootian et al. 2008). The negative and small values of free energy change (ΔG^0) were an indication of the spontaneous nature of the adsorption process. The negative values of standard enthalpy change (ΔH^0) for the intervals of temperatures were indicative of the exothermic nature of the adsorption process. Thermodynamic constants of adsorption obtained for Mn(II) and Fe(II) are summarized in Table 4.

Adsorption isotherms

Adsorption data for adsorbate concentration

Adsorption isotherms

The results of the adsorption experiments in this work were described by Freundlich, Langmuir and Temkin isotherms. Batch adsorption isotherms were carried out on sorption of manganese and iron using Ash-RH at room temperature. The adsorption isotherms data are illustrated in Figs. 9, 10, 11, 12, 13 and 14.

The result of Freundlich isotherm best fitted adsorption of Fe(II) on Ash-RH with correlation coefficient R^2 0.908 and moderately fitted the adsorption for Mn(II) with correlation coefficient R^2 0.758. The $1/n$ and K_f are obtained from the slope and intercept of the plot of ln (C_e) versus ln (q_e), the values of n and K_f are given in Table 5. The value of $1/n < 1$, for both metal ions implied favorable adsorption. The magnitude of K_f is a measure of the adsorbate on the adsorbent (Jalali et al. 2002; Igwe and Abia 2007). In this study, the sorption intensity on Mn(II) is higher than that of Fe(II).

The plots of C_e versus C_e/q_e for Mn(II) and Fe(II) are shown in Figs. 11, 12, the linear isotherm parameters q_m, b and the correlation coefficient are also given in the Table 6. Maximum sorption capacity, q_m of Fe(II) is 66.66 mg/g which is greater than that of Mn(II) of

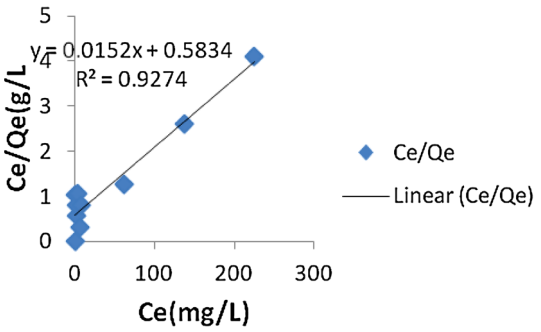

Fig. 12 Langmuir plot for sorption of Mn(II) ions on Ash-RH at pH 5, temp. 30 °C, adsorbent dose 0.1 g

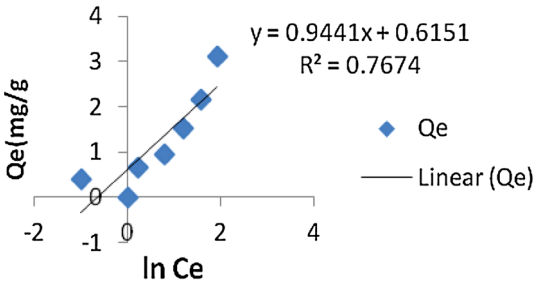

Fig. 13 Temkin plot for sorption of Mn(II) ions on Ash-RH at pH 5, temp. 30 °C, adsorbent dose 0.1 g

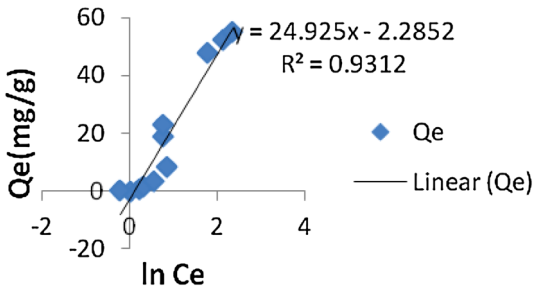

Fig. 14 Temkin plot for sorption of Fe(II) ions on Ash-RH at pH 5, temp. 30 °C, adsorbent dose 0.1 g

Table 5 Freundlich constants

Metal ions	$1/n$	log K_f	R^2	n	K
Mn(II)	0.259	0.159	0.758	3.861	1.4421
Fe(II)	0.916	0.031	0.908	1.091	1.0739

3.17 mg/g, this shows that the Ash-RH has greater ability to adsorb Fe(II) than Mn(II). Better fitting of the experimental data to Langmuir isotherm with regression coefficient of 0.948 and 0.927 for Mn(II) and Fe(II) indicate monolayer adsorption of Mn(II) and Fe(II) which may be due to homogeneous distribution of active sites onto adsorbent surface.

The plots of ln (C_e) versus q_e for Mn(II) and Fe(II) are shown in Figs. 13, 14 and the linear isotherm parameters

Table 6 Langmuir constants

Metal ions	$1/q_m$	$1/bq_m$	R^2	b	q_m	R_L
Mn(II)	0.315	2.361	0.948	0.1336	3.17	0.4281
Fe(II)	0.015	0.583	0.927	0.0257	66.66	0.7956

Table 7 Temkin constants

Metal ions	Slope = RT/B	Intercept = RT/B (InA)	R^2	B	A
Mn(II)	0.944	0.615	0.767	2686.2	4.64
Fe(II)	24.92	2.285	0.931	101.76	54.5

B, K_T and the correlation coefficient are given in Table 7. Constant B is related to heat of sorption, for Mn(II) it is 2,686.2 and 101.76 kJ/mol for Fe(II). Therefore, K_T which is the equilibrium binding constant for Fe(II) is greater than Mn(II), indicating a lower biomass metal ion potential for Mn(II) (Table 8).

The values of the linear regression coefficient (R^2) indicate that Langmuir, Freundlich and Temkin isotherms fit the equilibrium experimental data for Fe(II) while Langmuir best fit for Mn(II).

The direct comparison of adsorbent capacity of these rice husk ash with other sorbents reported in the literature is different due to varying experimental conditions employed in those studies. However, the solids in this study possess reasonable adsorption capacity in comparison with other adsorbents.

Adsorption kinetics

A good understanding of batch adsorption kinetics is needed for the design and operation of adsorption for Mn(II) and Fe(II) treatment. The nature of the Mn(II) and Fe(II) adsorption kinetic process depends on the physical or chemical characteristics of the adsorbent and also on the operating conditions. The kinetic data of Mn(II) and Fe(II) interactions with rice husk ash were, therefore, tested with different models such as pseudo-first order, pseudo-second order, intra-particle diffusion and liquid film diffusion model.

Only the pseudo-second order equation fitted best the kinetic data. The adsorption kinetic data for the various models are presented Figs. 15, 16.

Linear plot of t versus t/q_t (Figs. 15, 16) was used to determine the rate constants and correlation coefficients. For both Mn(II) and Fe(II) ions adsorption, the values of correlation coefficients of the data, were found to be very high ($R^2 > 0.99$). These values are shown in Table 9. The rate constant K obtained from slope of plot of t versus t/q_t, for Mn(II) is 0.292 mg/g min, as much greater than that of Fe(II)

Table 8 Comparison of results obtained in this study for the removal of Mn(II) with those of other adsorbents

Adsorbents	pH	Langmuir		Freundlich		References
		q (mg/g)	b (l/mg)	K_f (mg/g)	n (l/mg)	
Clay	4	3.80	0.0589	12.91	1.07	(Eba et al. 2010)
Clay	4	7.79	0.0415	12.32	1.27	(Eba et al. 2010)
Pristine Tamarindus fruit nut shell	4	122	0.0164	2.7	1.2	(Suguna et al. 2010)
Acid treated Tamarindus fruit nut shell	4	182	0.0218	4.6	1.2	(Suguna et al. 2010)
Activated carbon		27.78	0.2628	8.3645	2.72	(Chowdhury et al. 2011)
Activated carbon	7	0.2838	0.1067	0.3423	4.995	(Eba et al. 2010)
Activated carbon	7	0.4433	0.3087	0.1110	3.276	(Emmanuel and Veerabhadra 2009)
Rice husk ash	5	0.1336	3.17	3.861	1.4421	This study

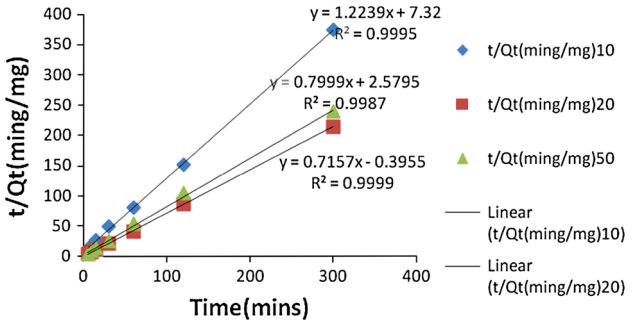

Fig. 15 Pseudo-second order kinetics for sorption of Ash-RH on Mn at pH 5, temp. 30 °C, adsorbent dose 0.1 g

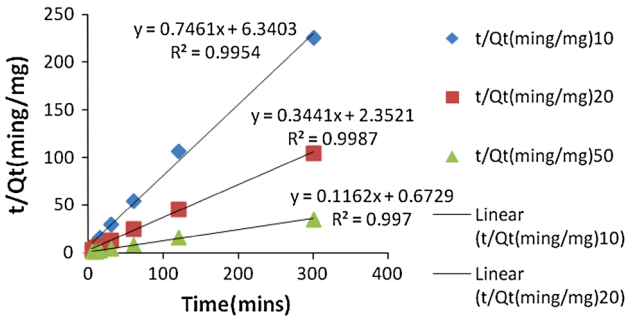

Fig. 16 Pseudo-second order kinetics for sorption of Ash-RH on Fe at pH 5, temp. 30 °C, adsorbent dose 0.1 g

which is 0.033 mg/g min at the same concentration of 10 ppm. This observation showed that Mn(II) ions adsorption takes place at higher rate than that of Fe(II) ions. The calculated q_e value from the pseudo-second order model is in good agreement with the experimental q_e value. This suggests that the sorption followed the pseudo-second order model (Muraleedharan and Venkobachar 1990; Park et al. 2006).

Characterization of Ash-RH using IR spectroscopy

The FTIR technique is an important tool to identify the characteristic functional groups (Fig. 17). The important peaks

Table 9 Pseudo second order constants extracted from Figs. 15, 16

Metal ions	Concn (mg/l)	Slope = $1/q_e$	Intercept	R^2	K_2 (g/mg/min)	q_e (cal)
Mn(II)	10	1.223	7.32	0.999	0.292	0.818
	20	0.799	2.579	0.998	0.965	1.251
	50	0.715	−0.395	0.999	0.075	1.40
Fe(II)	10	0.746	6.340	0.995	0.033	1.340
	20	0.344	2.352	0.998	0.026	2.91
	50	0.116	0.672	0.997	6.63×10^{-3}	8.621

extracted from the infrared (IR) spectra of the Ash-RH are summarized in Table 10. The different functional groups are of vital importance in understanding the adsorption process of the adsorbent. The infrared (IR) spectra of the samples had a broad band in the region of 3,433.41–3,446.91 cm^{-1} due to the surface O–H vibration. This band is due to the silanol, SiO–H groups and the HO–H vibration of the adsorbed water molecules bound to the silica surface (Kamath and Proctor 1998). This surface silanol groups are responsible for physically adsorbing water molecules and holding them in place by hydrogen bonding. The peak around 1,641.48–1,737.92 cm^{-1} corresponds to C=O stretching of aromatic groups that may be attributed to the hemicelluloses and lignin aromatic group. The C=C stretching vibrations between 1,514.17 and 1,656.91 cm^{-1} are indicative of alkenes and aromatic functional groups. The peaks around 1,471.74–1,462.09 cm^{-1} indicate the presence of CH_2 and CH_3. The peaks in the 1,163.11–1,315.5 cm^{-1} correspond to vibration of CO group in lactones. The peaks around 469.32–800 cm^{-1} indicate the presence of $–OCH_3$. All linkages present on the biomass surface are responsible for metal uptake process (Wong et al. 2000; Nadeem et al. 2006; Skoog et al. 2007).

Turbidity measurement

The result of turbidity measurement depicting the rate of sedimentation of rice husk particles as a function of time

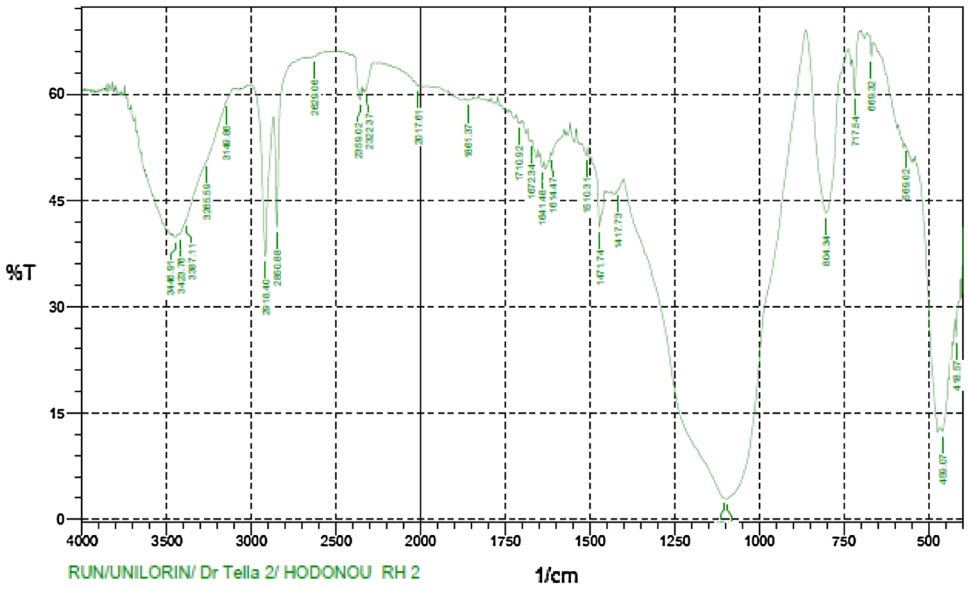

Fig. 17 IR spectra of the adsorbent Ash-RH A plot of turbidity of Ash-RH particles against time

Table 10 Functional groups presents in Ash-RH

Ash-RH	Assignment
3,446.91	–OH and Si–OH
2,918.4	C–H stretching of alkanes
1,641.48	C=O stretching of aromatic groups
1,510.31	C=C stretching of alkenes and aromatic
1,471.74	CH_2 and CH_3
1,105.25	CO group in lactones
459.07	$–OCH_3$

and pH are illustrated in Fig. 18. It is evident that turbidity decreases exponentially with time. It can be seen that the NTU decreases as the time increases. A practically clear supernatant was obtained within 15 min. So the suspension will, therefore, require continuous agitation of suspension during the adsorption process for the attachment of adsorptive metal ions on the adsorbents.

Desorption results

Desorption studies help to elucidate the nature of adsorption and recycling of the spent adsorbent. For desorption studies of the spent adsorbent, various concentrations of HCl solutions from 0.05 to 0.1 M were used. Maximum percents desorption obtained for men (II) and Fe(II) were 67 and 86 %, respectively, within 2 h for 0.1 M concentration of HCl. The results are illustrated in Fig. 19 for Ash-RH. It is important to note that at low concentration, the desorption solution was able to quantitatively remove the metal ions from the adsorbent, thereby reducing the expenses and waste generation.

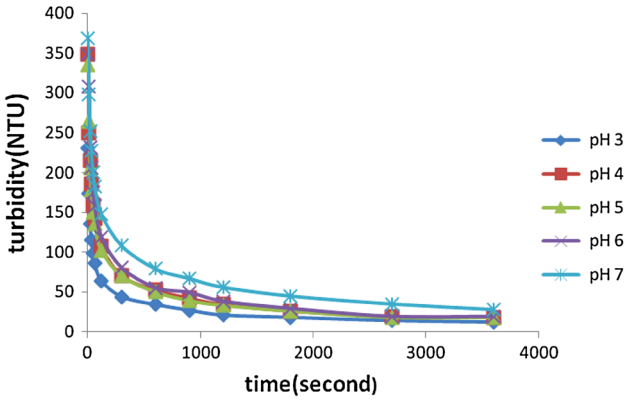

Fig. 18 Rate of sedimentation of Ash-RH with respect to time and pH

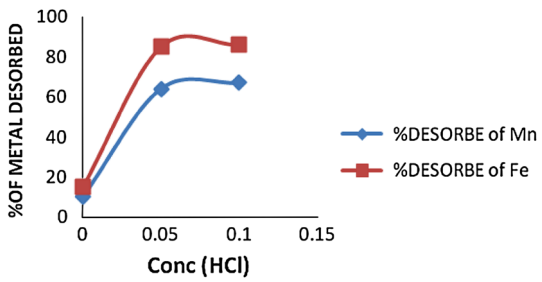

Fig. 19 A plot of percentage desorbed against molar concentration of HCl for Mn and Fe

Desorption index

The desorption index of Ash-RH with respect to Mn(II) and Fe(II) have been calculated and the values are summarized in Table 11.

Table 11 Desorption indices of Mn(II) and Fe(II)

HCl concentration (M)	Desorption index of Mn	Desorbed index of Fe
0.05	1.163	0.834
0.1	1.165	0.841
0.2	1.158	0.846

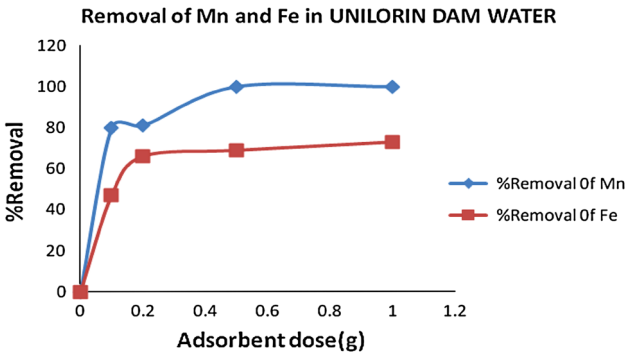

Fig. 20 A plot of percentage removal of Mn and Fe from Unilorin dam raw water against adsorbent dose pH = 3, temp = 30 °C, initial conc Mn(II) = 3.808 ppm and Fe^{2+}=6.28 ppm

The values of the desorption index (DI) were calculated for various concentrations of HCl from 0.05 to 0.2 M to evaluate the degree of reversibility of Mn(II)-Ash-RH and Fe(II)-Ash-RH sorption process. A sorption process is considered to be completely reversible when DI equals 1. The degree of irreversibility of a sorption reaction increases as DI value deviates from 1 (Adekola et al. 2012). In this study, the DI value for Mn(II)-Ash-RH ranged from 1.158 to 1.163, while that of Fe(II)–Ash-RH ranged from 0.834 to 0.846. The DI values are close to 1 which implies that the sorption process is practically reversible within the concentration range investigated.

Result of batch optimization conditions for the removal of Mn and Fe from untreated dam water

The results are illustrated in Fig. 20. It is interesting to note that 100 % of Mn(II) and nearly 70 % of Fe(II) were removed from the raw water after a contact time of 2 h and with adsorbent dose of 0.5 g.

Conclusion

The Ash-RH (rice husk ash) was found to be an effective biosorbent for the removal of Mn(II) and Fe(II) from an aqueous solution. The study showed that the initial concentration, contact time, the adsorbents dose, temperature and pH of the solution influenced the adsorption process. Thermodynamic studies showed that the adsorption process was feasible and spontaneous and exothermic in nature. A good fit of the adsorption data into the Langmuir isotherm confirmed monolayer adsorption for both metals Mn and Fe. The prepared rice husk effectively removed manganese and iron from the raw water of the University of Ilorin dam.

References

Abdullah AH, Kassim A, Zainal Z, Zobir Hussien M, Faujan Ahmad D, Wool O (2001) Preparation & characterization of activated carbon from gelam wool bark. Malays J Anal Sci 7(1):65–68

Adekola FA, Abdulssalam N, Adegoke HI, Adesola AM, Adekeye JID (2012) Removal of Pb(II) from aqueous solution by Natural and synthetic Calcites. Bull Chem Soc Ethiopia 26(2):195–210

Annadurai G, Chellapandian M, Krishnan MRV (1997) Adsorption of basic dye from aqueous solution by chitosan: equilibrium studies. Indian J Env Prot 17(2):95–98

Bhattacharyya KG, Gupta Sen S (2006) Pb(II) uptake by kaolinite and montmorillonite in aqueous medium influence of acid activation of the clays. Coll Surf A Physiochem Eng Aspects 277:191–200

Chowdhury ZZ, Zain SM, Khan RA, Ahmad AA, Islam MS, Arami-Niya A (2011) Application of central composite design for preparation of Kenaf fiber based activated carbon for adsorption of Manganese (II) ion. Int J Phys Sci 6(31):7191–7202

Danis U, Gurses A, Caupolat N (1999) Removal of some azo dyes from wastewater using PAC as adsorbent. Fres Env Bull 8:358–365

Dubinin MM, Radushkevich LV (1947) Equation of the Characteristic curve of activated charcoal. Chemisches Zentralblatt 1:875–890

Eba F, Gueu S, Mvongbote EA, Ondo JA, Yao BK, Ndong Nlo J, Kouya Bibouta R (2010) Evaluation of the adsorption capacity of the natural clay from BiKougou (Gabon) to remove Mn(II) froms aqueous solution. Int J Eng Sci Technol 2(10):5001–5016

El-Said AG, Badawy NA, Garamon SE (2010) Adsorption of Cadmium (II) and Mercury (II) onto natural adsorbent rice husk ash (RHA) from aqueous solutions: study in single and binary system. J Am Sci 6(12):400–409

Emmanuel KA, Veerabhadra Rao A (2009) Comparative study on adsorption of Mn(II) from aqueous solutions on various activated carbons. E-J Chem 6(3):693–704

Hall KR, Eggleton LC, Acrivos A, Vermeulan TH (1966) Pore- and solid-diffusion kinetics in fixed bed adsorption under constant-pattern conditions. Ind Eng Chem Fundam 5(2):212–223

Ho YS, McKay G (2002) Application of kinetic models to the sorption of Cu (II) onto Peat. Adsorpt Sci Technol 20(8): 797–815

Ho YS, Wase DAJ, Forster CF (1996) Kinetics studies of competitive heavy metal adsorption by *Sphagnum moss* peat. Environ Technol 17:71–77

Hutson ND, Yang RT (1997) Theoretical basis for the Dubinin-Radushkevich (D-R) adsorption isotherm equation. Adsorption. 3:189–195

Igwe JC, Abia AA (2007) Equilibrium sorption isotherm studies of Cd (II), Pb(II) and Zn (II) ion detoxification from waste water using unmodified and EDTA—modified Maize husk. Electron J Biotechnol 10(4):102–125

Jahn SAA (1988) Using Moringa Oleifera seeds as coagulant developing countries. J Am Water Works Assoc 6:43–50

Jalali R, Ghafourian H, Asef Y, Davarpanah SJ, Sepehr S (2002) Removal and recovery of lead using non-living biomass of marine algae. J Hazard Mater 92:253–262

Kalavathy MH, Miranda LR (2010) Moringa Oleifera—a solid phase extractant for the removal of copper and zinc from aqueous solutions. Chem Eng J 158:188–199

Kamath SR, Proctor A (1998) Silica gel from rice hull ash: preparation and characterization. Cereal Chem 75:484–487

Khan AR, Tahir H, Uddin F, Hammed U (2005) Adsorption of methylene blue from aqueous solution on the surface of wool fibre and cotton fibre. J Appl Sci Environ Manag 9(2):29–35

Lakshminarayanan KC, Rao K, Krishna A (1994) Colour removal from the dyestuff industry effluent using activated carbon. Indian J Chem Technol 1:13–19

Laurence MH, Christopher JM (1989) Experimental organic chemistry: principles and practice (Illustrated Ed.). Wiley-Blackwell, New York, p. 292

Malakootian M, Almasi A, Hanoi H (2008) Pb and Co removal from paint industries effluent using wood ash. Int J Environ Sci Technol 5(2):217–222

Mckay G, Ho YS (1999) Pseudo-second order model for sorption process. Biochemistry 34:451–465

Mohan S, Karthikeyan J (1997) Removal of lignin and tannin colour from aqueous solution by adsorption onto activated. Environ Pollut 97:183–187

Muraleedharan TR, Venkobachar C (1990) Mechanism of biosorption of Cu (II) by *Ganoderma lucidum*. Biotechnol Bioeng 35:320–325

Nadeem M, Mahmood A, Shahid SA, Shah SS, Khalid AM, McKaye G (2006) Sorption of lead from aqueous solution by chemically modified carbon adsorbents. J Hazard Mater B138:604–613

Park D, Yun YS, Lim SR, Park JM (2006) Kinetic analysis and mathematical modeling of Cr(VI) removal in a different reactor parked with *ecklonia* biomass. J Microbiol Biotechnol 16(2): 1720–1727

Sari A, Mendil D, Tuzen M, Soylak M (2008) Biosorption of Cd(II) and Cr(II) from aqueous solution by moss (*Hylocomium splendens*) biomass: equilibrium, kinetic and thermodynamic studies. Chem Eng J 144:1–9

Sari A, Tuzen M (2009) Kinetic and equilibrium studies of biosorption of Pb(II) and Cd (II) from aqueous by macrofungus (*Amanita rubescens*) biomass. J Hazard Mater 164:1004–1011

Singh DB, Prasad G, Rupainwar DC, Singh VN (1988) As (III) removal from aqueous solution by adsorption. Water Air Soil Poll 42:373–386

Spellman FR (2001) Handbook for waterworks operator certification, vol 2. Technomic Publishing Company Inc., Lancaster, pp 6–11, 81–83

Suguna MS, Siva Kumar N, Venkata Subbaiah M, Krishnaiah A (2010) Removal of divalent manganese from aqueous solution using Tamarindus indica fruit nut shell. J Chem Pharm Res 2(1):7–20

Temkin M, Pyzhev JAV (1940) Kinetics of ammonia synthesis on promoted iron catalysts. Acta Physiochem. 12:217–222

Voudrias E, Fytianosand F, Bozani E (2002) Sorption description isotherms of dyes from aqueous solutions and waste waters with different sorbent materials, global nest. Int J 4(1):75–83

Wong JPK, Wong YS, Tam NFY (2000) Ni(II) biosorption by two choeral species, *C. vulgaris* (a commercial species) and *C. miniata* (a local isolate). Bioresour Technol 73:133–137

Xiao B, Thomas KM (2004) Competitive adsorption of aqueous metal ions on an oxidized nanoporous activated carbon. Langmuir Am Chem Soc 20:4566–4578